

available at [www.sciencedirect.com](http://www.sciencedirect.com)journal homepage: [www.elsevier.com/locate/biochempharm](http://www.elsevier.com/locate/biochempharm)

# Sarcoplasmic reticulum $\text{Ca}^{2+}$ release channel ryanodine receptor ( $\text{RyR}_2$ ) plays a crucial role in aconitine-induced arrhythmias

Min Fu<sup>a,b</sup>, Ru-Xin Li<sup>a</sup>, Li Fan<sup>c</sup>, Guo-Wei He<sup>c</sup>, Kent L. Thornburg<sup>d,\*\*</sup>, Zhao Wang<sup>a,\*</sup>

<sup>a</sup> School of Medicine and Department of Biological Sciences and Biotechnology, Tsinghua University, Beijing 100084, People's Republic of China

<sup>b</sup> Beijing University of Chinese Medicine, Beijing 100029, People's Republic of China

<sup>c</sup> Cardiovascular Research, Starr Academic Center for Cardiac Surgery, Heart & Vascular Institute, Providence St. Vincent Medical Center, Portland, OR 97225, USA

<sup>d</sup> Heart Research Center, L464, Oregon Health & Science University, Portland, OR 97239, USA

## ARTICLE INFO

### Article history:

Received 2 December 2007

Accepted 22 February 2008

### Keywords:

$\text{RyR}_2$

Knockdown

Aconitine

Arrhythmia

Excitation–contraction coupling

## ABSTRACT

The present study established a model of  $\text{RyR}_2$  knockdown cardiomyocytes and elucidated the role of  $\text{RyR}_2$  in aconitine-induced arrhythmia. Cardiomyocytes were obtained from hearts of neonatal Sprague–Dawley rats. siRNAs were used to down-regulate  $\text{RyR}_2$  expression. Reduction of  $\text{RyR}_2$  expression was documented by RT-PCR, western blot, and immunofluorescence.  $\text{Ca}^{2+}$  signals were investigated by measuring the relative intracellular  $\text{Ca}^{2+}$  concentration, spontaneous  $\text{Ca}^{2+}$  oscillations, caffeine-induced  $\text{Ca}^{2+}$  release, and L-type  $\text{Ca}^{2+}$  currents. In normal cardiomyocytes, steady and periodic spontaneous  $\text{Ca}^{2+}$  oscillations were observed, and the baseline  $[\text{Ca}^{2+}]_i$  remained at the low level. Exposure to 3  $\mu\text{M}$  aconitine increased the frequency and decreased the amplitude of  $\text{Ca}^{2+}$  oscillations; the baseline  $[\text{Ca}^{2+}]_i$  and the level of caffeine-induced  $\text{Ca}^{2+}$  release were increased but the L-type  $\text{Ca}^{2+}$  currents were inhibited after application of 3  $\mu\text{M}$  aconitine for 5 min. In  $\text{RyR}_2$  knockdown cardiomyocytes, the steady and periodic spontaneous  $\text{Ca}^{2+}$  oscillations almost disappeared, but were re-induced by aconitine without affecting the baseline  $[\text{Ca}^{2+}]_i$  level; the level of caffeine-induced  $\text{Ca}^{2+}$  release was increased but L-type  $\text{Ca}^{2+}$  currents were inhibited. Alterations of  $\text{RyR}_2$  are important consequences of aconitine-stimulation and activation of  $\text{RyR}_2$  appear to have a direct relationship with aconitine-induced arrhythmias. The present study demonstrates a potential method for preventing aconitine-induced arrhythmias by inhibiting  $\text{Ca}^{2+}$  leakage through the sarcoplasmic reticulum  $\text{RyR}_2$  channel.

© 2008 Elsevier Inc. All rights reserved.

\* Corresponding author. Tel.: +86 10 6277 2240; fax: +86 10 6277 2675.

\*\* Corresponding author. Tel.: +1 503 494 2305; fax: +1 503 494 8550.

E-mail addresses: [thornbur@ohsu.edu](mailto:thornbur@ohsu.edu) (K.L. Thornburg), [zwang@tsinghua.edu.cn](mailto:zwang@tsinghua.edu.cn) (Z. Wang).

Abbreviations:  $\text{RyR}_2$ , type 2-ryanodine receptor; KD, knockdown; e-c coupling, excitation–contraction coupling; ACO, aconitine; SR, sarcoplasmic reticulum; siRNA, small interfering RNA.

0006-2952/\$ – see front matter © 2008 Elsevier Inc. All rights reserved.

doi:10.1016/j.bcp.2008.02.027

## 1. Introduction

Aconite tuber, roots of aconite (*Aconitum carmichaeli* or *A. kusnezofii*), is an important oriental herbal medicine used for centuries in China and other countries to therapeutically increase the peripheral temperature, relieve rheumatic pain and treat neurological disorders [1]. The pharmacological effects of Aconitum alkaloids include positive inotropic effects, analgesic, anti-inflammatory, and antirheumatic activity as well as neurotransmission actions [2–4]. Aconitine and its structurally related analogs are known to injure both the central nervous system and the heart [5]. Its cardiotoxicity consists primarily of arrhythmic effects and it has been used as an experimental tool to induce tachyarrhythmias in animal models [6]. In spite of its potential toxic effects, aconitine remains a popular home remedy for several ailments in China. Although most mechanisms postulated for aconitine toxicity focus on voltage-dependent  $\text{Na}^+$  channels, little is known about its interaction with intracellular  $\text{Ca}^{2+}$  signals and  $\text{Ca}^{2+}$  handling proteins that regulate the cardiac excitation–contraction coupling (e–c coupling) system. We have shown previously that aconitine impairs the contractile function by disrupting the intracellular  $\text{Ca}^{2+}$  homeostasis in the cardiac e–c coupling of cultured cardiomyocytes and stimulating up-regulation of the type 2-ryanodine receptor ( $\text{RyR}_2$ ) level significantly [7]. The present study was therefore designed to establish a model of  $\text{RyR}_2$  knockdown (KD) cardiomyocytes and elucidate the role of  $\text{RyR}_2$  in aconitine-induced arrhythmia.

In cardiac muscle, the intracellular  $\text{Ca}^{2+}$  stores and the sarcoplasmic reticulum (SR)  $\text{Ca}^{2+}$  release play prominent roles in cardiac contractile activation and relaxation [8–10].  $\text{Ca}^{2+}$  release from SR through the cardiac  $\text{RyR}_2$  channel is a fundamental event in cardiac muscle contraction, which is triggered by calcium-induced calcium release (CICR) [11]. Alterations in the sensitivity of  $\text{RyR}_2$  to  $\text{Ca}^{2+}$  release activation have been implicated in diseases including malignant hyperthermia and heart failure [12–14]. Mutations in  $\text{RyR}_2$  that are suspected to cause defective  $\text{Ca}^{2+}$  channel function and aberrant intracellular  $\text{Ca}^{2+}$  signals have recently been identified in catecholaminergic polymorphic ventricular tachycardia (CPVT) and arrhythmogenic right ventricular dysplasia (ARVD) patients [15]. Cardiomyocytes in  $\text{RyR}_2$  gene knock-out (KO) mice show a decrease in the rate of spontaneous diastolic depolarization and an absence of calcium sparks [16].

We report here that  $\text{RyR}_2$  gene expression was strongly reduced in cultured neonatal rat cardiomyocytes by exogenous transcription of small interfering RNAs (siRNAs). Moreover, we examined the effects of aconitine on the relative intracellular  $\text{Ca}^{2+}$  concentration, spontaneous  $\text{Ca}^{2+}$  oscillations, caffeine-induced  $\text{Ca}^{2+}$  release and L-type  $\text{Ca}^{2+}$  channel currents in control and  $\text{RyR}_2$  KD cardiomyocytes.

## 2. Materials and methods

### 2.1. Animals and chemicals

Cardiomyocytes were obtained by dissociating hearts of neonatal Sprague–Dawley rats (1–3 days old). The experi-

mental protocol for animals was approved by the Medical Ethical Committee of Tsinghua University. Aconitine (content  $\geq 98\%$ ) was purchased from the National Institute for the Control of Pharmaceutical & Biological Products (China).

### 2.2. $\text{RyR}_2$ gene knockdown techniques

#### 2.2.1. Preparation of siRNAs for targeting on $\text{RyR}_2$ gene

siRNAs were designed by Ambion (Ambion Inc., USA) according to the guidelines for effective knockdown. Three double-stranded siRNAs for targeting rat  $\text{RyR}_2$  gene were as follows: target 1 for  $\text{RyR}_2$  (siRNA1), 5'-CCUUGAACAGAAUCUAAGtt-3' (sense) and 5'-CUUAGAUUCUGUUAAGGtg-3' (antisense); target 2 for  $\text{RyR}_2$  (siRNA2), 5'-CCCUCAGAGAUCAAAGAAAtt-3' (sense) and 5'-UUUCUUUGAUCUCUGAGGGtg-3' (antisense); target 3 for  $\text{RyR}_2$  (siRNA3), 5'-GCCAUGAAAAGAGUUGAUCtt-3' (sense) and 5'-GAUCAACUCUUUCAUGGctt-3' (antisense). The positive control siRNAs (anti-GAPDH siRNA) were purchased from Ambion. All siRNAs were provided in a freeze-dried, preannealed, HPLC-purified form ( $>80\%$ ). 20 nmol of annealed siRNA was resuspended into 200  $\mu\text{l}$  RNA-free  $\text{ddH}_2\text{O}$  as a stock solution at the concentration of 100  $\mu\text{M}$ , and stored at  $-70^\circ\text{C}$  until required.

#### 2.2.2. Cell cultures and siRNA transfection

Primary cardiomyocyte cultures were obtained as previously described [17]. Cells were seeded into six-well plates at a final density of  $1.5\text{--}3 \times 10^5$  cells per well in DMEM/F12 media (Invitrogen Corporation, USA) supplemented with 10% fetal bovine serum (FBS) (Hyclone Laboratories Inc., USA) for 3 days under normal growth conditions ( $37^\circ\text{C}$ , 91% humidity and 5%  $\text{CO}_2$ ). All siRNAs were transfected into cardiomyocytes monolayers by using the siPORT<sup>TM</sup> NeoFX<sup>TM</sup> lipid-based reagent for reverse transfection (Ambion Inc., USA) according to the transfection protocol. After 6 h of transfection, the complexes were removed from the six-well plates. 2 ml fresh media containing 10% FBS was added to the plates. After 6 and 72 h, cardiomyocytes were used for subsequent experiments, each of which was performed at least three times. The controls were analyzed in parallel.

To optimize the contribution of the siRNA amount and the siPORT<sup>TM</sup> NeoFX<sup>TM</sup> volume to transfection efficiency in six-well plates, total volume of siRNA (2  $\mu\text{M}$ ) was varied between 1.25 and 37.5  $\mu\text{l}$ , and siPORT<sup>TM</sup> NeoFX<sup>TM</sup> volume was varied between 2 and 6  $\mu\text{l}$  per well. The cytotoxicity was evaluated by MTT assays. Down-regulation of  $\text{RyR}_2$  expression was identified by RT-PCR, western blot, and immunofluorescence analyses.

#### 2.2.3. RT-PCR analyses

Total cellular RNA was extracted by PUREGENE<sup>TM</sup> RNA isolation kit (Gentra Systems, USA). Spectrophotometry at 260 and 280 nm was performed to measure the amount and purity of RNA. The specific primers used for RT-PCR are described in Ref. [7]. The GAPDH primer was as follows: sense, 5'-TTGGCCGTATTGGCCGC-3'; antisense, 5'-GTGCCATTGAAC-TTGCCGTG-3'. The PCR condition was  $95^\circ\text{C}$  for 1 min 30 s,  $94^\circ\text{C}$  for 30 s,  $52\text{--}60^\circ\text{C}$  for 40 s, and  $72^\circ\text{C}$  for 30 s, 35 cycles, with a final extension for 5–7 min at  $72^\circ\text{C}$ . In all experiments, the threshold count values were normalized to the internal control

of GAPDH before calculating the changes for all of the genes. The products were separated by 1.5% agarose gel stained with ethidium bromide (EB). Intensity of the DNA bands was analyzed using the Totallab TL100 software (Nonlinear Inc., USA).

#### 2.2.4. Western blot analyses

Protocols described in reference 18 were followed [18]. Protein samples (120  $\mu$ g of total protein per lane) were separated by 5% SDS-PAGE gels for RyR and transferred to PVDF membranes. The membranes were probed with the monoclonal anti-RyR (1:2500, MA3-925) (Affinity Bioreagents, USA). A peroxidase-conjugated goat anti-mouse IgG was used as a secondary antibody (1:5000) (Affinity Bioreagents, USA).  $\beta$ -Actin was used as the internal standard for analysis of the protein. Signals were detected using the super signal ECL substrate (Pierce Biotechnology Inc., USA). The Totallab TL100 software was used to analyze the protein bands (Nonlinear Inc., USA).

#### 2.2.5. Immunofluorescence assays

For immunofluorescence assays, cardiomyocytes were fixed with the mixture of methanol and acetone (v/v, 1:1) and blocked in 10% horse serum for 30 min at 37 °C. They were then incubated with the primary monoclonal anti-RyR (1:1000, MA3-925) (Affinity Bioreagents, USA) for 1 h at 37 °C, followed by goat anti-mouse IgG-FITC (1:100) secondary antibody (Santa Cruz Biotechnology Inc., USA) in dark chamber for 30 min at 37 °C. After that, cells were subsequently stained with PI (5  $\mu$ g/ml, PBS) for 5 min and detected using a ZEISS LSM510 META laser-scanning confocal microscope (MIC Bergen, USA). Fluorescence recordings were done with either 488 nm laser excitation (520LP emission) or 543 nm laser excitation (580LP emission).

### 2.3. Assays of $\text{Ca}^{2+}$ signals

#### 2.3.1. Assays of the spontaneous $\text{Ca}^{2+}$ oscillations and the relative intracellular $\text{Ca}^{2+}$ concentration by $\text{Ca}^{2+}$ imaging

$\text{Ca}^{2+}$  imaging experiments were performed to measure the spontaneous  $\text{Ca}^{2+}$  oscillations and the relative intracellular  $\text{Ca}^{2+}$  concentration in control and RyR<sub>2</sub> KD cardiomyocytes with aconitine-stimulation [19]. Cardiomyocytes were inoculated in 35 mm dishes (MatTek Corporation, USA) and loaded with 5  $\mu$ M fluo-3 AM (Sigma Chemical Co., USA). Intracellular fluo-3 AM was excited by a DG-4 quartz lamp filtered at 488 nm, and emission wavelengths were monitored with a 520 nm long-pass filter in 37 °C perfusion solution (in mM: 145 NaCl, 5.4 KCl, 0.5  $\text{MgCl}_2$ , 1.2  $\text{CaCl}_2$ , 5 HEPES, 5.5 Glucose, 0.3  $\text{NaH}_2\text{PO}_4$ , pH 7.4) [20]. Rapid scanning of the observation field (5 s/scan) was used to minimize photo-oxidation artifacts. The images were recorded by a CoolSNAP fx CCD camera (Roper Scientific, USA).  $\text{Ca}^{2+}$  oscillations were recorded and analyzed using MetaFluor software (Universal Imaging Corporation, USA).

#### 2.3.2. Assessments content of SR $\text{Ca}^{2+}$ release stimulated by caffeine

To evaluate the SR  $\text{Ca}^{2+}$  loading state, caffeine (20 mM) was applied to stimulate  $\text{Ca}^{2+}$  release from SR. After the relative intracellular free  $\text{Ca}^{2+}$  concentration ( $[\text{Ca}^{2+}]_i$ ) transients of the fluo-3 AM loaded cardiomyocytes became stable, a rapid pulse of 20 mM caffeine (200 ms) was applied to the cardiomyocytes

via a micropipette ( $\sim 4 \mu\text{m}$  at tip). The micropipette was placed downstream with respect to the superfusate flow, which prevented caffeine leaking out of the pipette from diffusing to the cardiomyocytes. Baseline values for  $[\text{Ca}^{2+}]_i$  were measured in individual cells. Resting and peak  $[\text{Ca}^{2+}]_i$  during caffeine application were each converted to total cytosolic  $\text{Ca}^{2+}$  taking into account estimated  $\text{Ca}^{2+}$  binding at high and low affinity sites. The difference ( $\Delta[\text{Ca}^{2+}]_i$ ) was taken as the total level of caffeine-induced  $\text{Ca}^{2+}$  release. Cells without treatment were initiated by a puff of caffeine to induce SR  $\text{Ca}^{2+}$  release. After washed out the caffeine with perfusion solution, cells were treated with 3  $\mu\text{M}$  aconitine for 5 min, and then initiated with the puff of caffeine to induce SR  $\text{Ca}^{2+}$  release.

#### 2.3.3. L-type $\text{Ca}^{2+}$ currents assay by patch clamp

Intracellular  $\text{Ca}^{2+}$  currents were recorded using the whole-cell patch clamp technique. The culture media was replaced with the external solution (in mM: 120 NaCl, 5 KCl, 1  $\text{MgCl}_2$ , 3.6  $\text{CaCl}_2$ , 10 HEPES, 20 TEA, 0.001 TTX, pH 7.4 (TEAOH)) before recording. The patch pipettes (4–6 M resistance) were filled with the internal solution (in mM: 120 CsCl, 3  $\text{MgCl}_2$ , 5 HEPES, 10 EGTA, 5 MgATP, pH 7.4 (CsOH)) [21]. Whole-cell patch clamp recordings were made at room temperature (21–23 °C) with the Axopatch-200B amplifier (Axon Instruments, USA) in conjunction with pClamp9 software (Axon Instruments, USA). Cardiomyocytes were clamped at  $-40 \text{ mV}$  and step depolarized to  $+50 \text{ mV}$  in 10 mV increments.  $\text{Ca}^{2+}$  current recordings were filtered with a current filter at 5 kHz.

### 2.4. Statistical analyses

Data were presented as mean  $\pm$  S.E. Differences between means were determined using the Student's t-test for paired observations. Differences were considered statistically significant when  $p$ -value  $< 0.05$ .

## 3. Results

### 3.1. Maximal reduction of RyR<sub>2</sub> mRNA level was achieved by exogenous transcription of siRNA3 48 h after transfection

In order to examine the silencing specificity of the three siRNAs in primary cultured cardiomyocytes from hearts of neonatal SD rats (1–3 days), mRNA levels of RyR<sub>2</sub> were investigated by RT-PCR. Transfection of cardiomyocytes with the siRNA3 template led to significant reduction of mRNA level of RyR<sub>2</sub>.

To further examine siRNA specificity, reduction of RyR<sub>2</sub> expression in cardiomyocytes after delivery of siRNA3 for 6–72 h was documented by mRNA level (semiquantitative RT-PCR) paralleled with the corresponding protein expression (western blot) (Fig. 1A and B). Changes in mRNA and protein levels of RyR<sub>2</sub> were noted in cardiomyocytes with siRNA transfection after 24 h. We can also see that changes in mRNA and protein levels after 48–72 h were more significant than other time point. But it was shown in MTT assays that cytotoxicity of the cardiomyocytes with transfection after 72 h was more obvious than that in cardiomyocytes with transfection after 48 h, so in the subsequent experiments, we use the KD cardiomyocytes with transfection after 48 h.

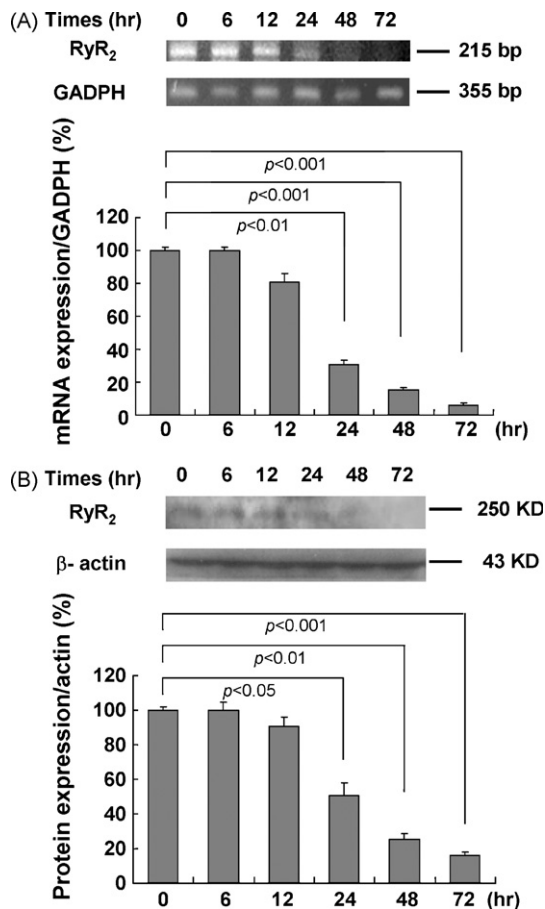


**Fig. 1 – Effects of siRNA3 target on mRNA and protein levels of RyR<sub>2</sub> in rat primary cardiomyocytes with transfection after 6–72 h tested by RT-PCR and western blot. (A) Changes in mRNA levels of RyR<sub>2</sub> in cardiomyocytes with siRNA3 transfection after 6–72 h. GAPDH served as an internal control for analysis of the PCR productions. (B) Changes in protein expressions of RyR<sub>2</sub> in cardiomyocytes with siRNA3 transfection after 6–72 h.  $\beta$ -Actin was used as a standard for analysis of the protein samples. Data are presented as the mean  $\pm$  S.E. Differences were considered statistically significant when  $p$ -value  $< 0.05$ ,  $t$ -test,  $n = 4$ .**

Of the three siRNAs, the maximal silencing effect of RyR<sub>2</sub> was achieved with the siRNA3 targeting rat RyR<sub>2</sub> gene from 2137 to 2155 bp. The silencing effects of siRNA1 and siRNA2 targeting 1850–1868 bp and 1902–1920 bp, respectively, were less obvious than that of siRNA3 (XM\_341548). The optimal siRNA amount and siPORT<sup>TM</sup> NeoFX<sup>TM</sup> volume that yielded the best transfection efficiency in six-well plates were under the following conditions: total volume of media is 1 ml, total volume of siRNA (2  $\mu$ M) is 5  $\mu$ l, and the siPORT<sup>TM</sup> NeoFX<sup>TM</sup> volume is 4  $\mu$ l per well.

### 3.2. The mRNA and protein levels of RyR<sub>2</sub> were increased by aconitine

To examine the effect of aconitine on RyR<sub>2</sub>, RT-PCR, western blot, and immunofluorescence were used to examine RyR<sub>2</sub>

expression. As illustrated in Fig. 2A and B, mRNA and protein levels were increased both in control and KD cardiomyocytes induced by 3  $\mu$ M aconitine for 0.5 h. We can also see that alteration of RyR<sub>2</sub> expression in KD cardiomyocytes is more obvious rather than that in control cardiomyocytes. (mRNA level: from  $100.05 \pm 6.31$  to  $182.51 \pm 17.85\%$  in CN cardiomyocytes and from  $22.76 \pm 8.42$  to  $51.89 \pm 12.33\%$  in KD cardiomyocytes, respectively; protein level: from  $100.08 \pm 6.04$  to  $142.39 \pm 9.61\%$  in CN cardiomyocytes and from  $35.12 \pm 11.3$  to  $62.38 \pm 6.74\%$  in KD cardiomyocytes, respectively.)

Immunostaining was used to localize RyR<sub>2</sub> in cardiomyocytes (Fig. 2C). Fluorescence in cardiomyocytes stained with primary anti-RyR and FITC-labeled secondary antibodies was noted in control cardiomyocytes with cytosolic prominence likely caused by active RyR<sub>2</sub> expression. We observed the reduction of RyR<sub>2</sub> expression in all cardiomyocytes visible in the field, which indicates a very efficient siRNA delivery 48 h after transfection. We can also see in Fig. 2C that, consistent with RT-PCR and western blot results, RyR<sub>2</sub> fluorescence was significantly increased after exposure to 3  $\mu$ M aconitine for 0.5 h in RyR<sub>2</sub> KD cardiomyocytes.

### 3.3. Aconitine-induced recovery of spontaneous Ca<sup>2+</sup> oscillations without affecting the baseline [Ca<sup>2+</sup>]<sub>i</sub> in RyR<sub>2</sub> KD cardiomyocytes

We used digital imaging technique to explore the effects of aconitine on spontaneous Ca<sup>2+</sup> oscillations and the relative intracellular Ca<sup>2+</sup> concentration (baseline [Ca<sup>2+</sup>]<sub>i</sub>) in control and RyR<sub>2</sub> KD cardiomyocytes (Fig. 3A and B). In control cardiomyocytes, steady and periodic spontaneous Ca<sup>2+</sup> oscillations were observed, and the baseline [Ca<sup>2+</sup>]<sub>i</sub> remained at low level. Application of 3  $\mu$ M aconitine resulted in a significant increase in the frequency (nearly 2-fold higher, from  $7.25 \pm 0.25$  to  $13.75 \pm 0.35$ ,  $p < 0.05$ ) and a decrease in the amplitude of spontaneous Ca<sup>2+</sup> oscillations (from  $159.41 \pm 12.72$  to  $113.34 \pm 3.34$   $\Delta F/F_0\%$ ,  $p < 0.05$ ). A significant elevation of the baseline [Ca<sup>2+</sup>]<sub>i</sub> (from  $11.38 \pm 1.07$  to  $82.14 \pm 13.66$   $\Delta F/F_0\%$ ,  $p < 0.01$ ) was also observed.

In contrast, in RyR<sub>2</sub> KD cardiomyocytes, steady and periodic spontaneous Ca<sup>2+</sup> oscillations disappeared completely. Interestingly, application of 3  $\mu$ M aconitine re-induced spontaneous Ca<sup>2+</sup> oscillations (frequency: from  $0.5 \pm 0.29$  to  $4.4 \pm 0.2$ ,  $p < 0.01$ ; amplitude: from  $65.52 \pm 6.66$  to  $73.45 \pm 7.42$   $\Delta F/F_0\%$ ) without affecting the baseline [Ca<sup>2+</sup>]<sub>i</sub> level ( $15.23 \pm 3.38$  vs.  $17.93 \pm 1.36$   $\Delta F/F_0\%$ ) (Fig. 3D–F).

### 3.4. The level of caffeine-induced Ca<sup>2+</sup> release in the cardiomyocytes was increased by aconitine

The SR Ca<sup>2+</sup> release from the SR was estimated by the traditional caffeine puff. The Ca<sup>2+</sup> content released from SR during the caffeine contracture was measured as  $\Delta F/F_0\%$ . Superimposed Ca<sup>2+</sup> transients in control and RyR<sub>2</sub> KD cardiomyocytes were performed (Fig. 4A and B). It was shown that Ca<sup>2+</sup> transients were relatively smaller in RyR<sub>2</sub> KD cardiomyocytes than those in control cardiomyocytes ( $164.25 \pm 33.29$  vs.  $83.89 \pm 28.36$   $\Delta F/F_0\%$ ). The alterations of transient amplitudes, however, were amplified significantly in both of these two kinds of cardiomyocytes when the caffeine



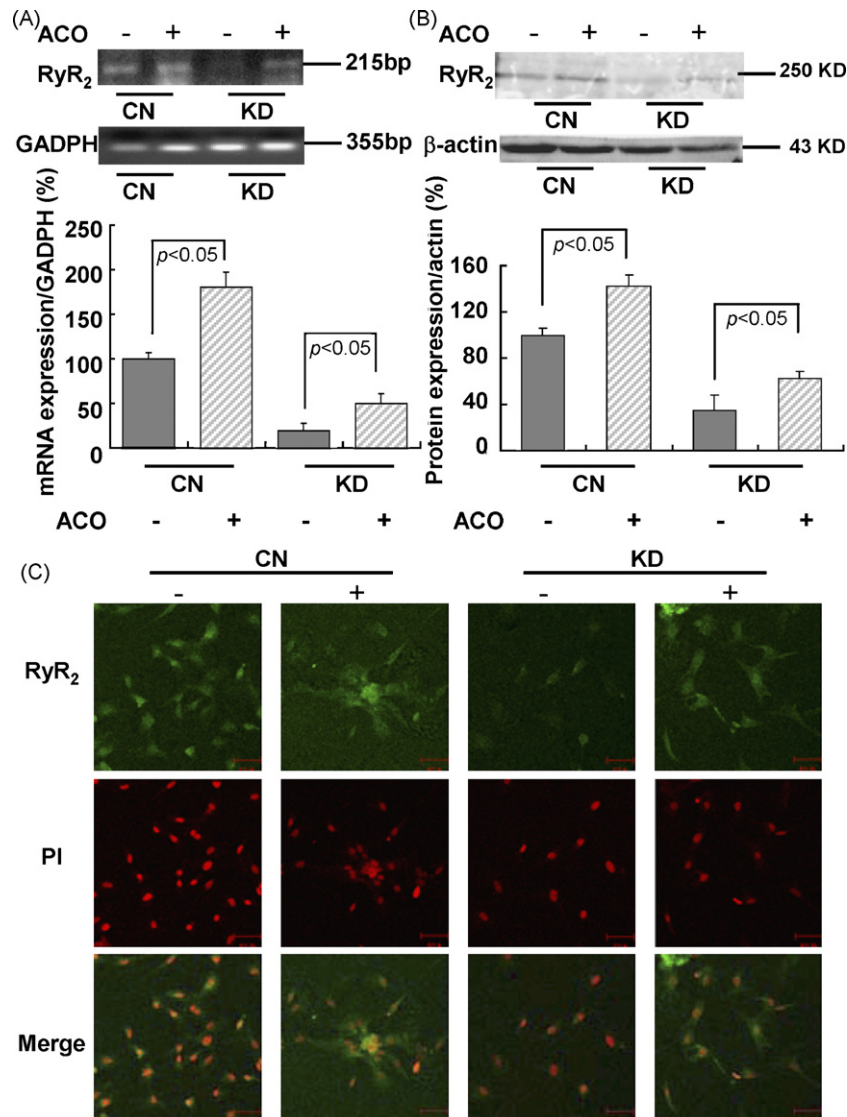


**Fig. 2 – Effects of aconitine on mRNA and protein levels of RyR<sub>2</sub> in control cardiomyocytes and knockdown cardiomyocytes (with siRNA3 transfection after 48 h) tested by RT-PCR, western blot, and immunostaining. (A and B) Changes in mRNA and protein levels of RyR<sub>2</sub> in CN and KD cardiomyocytes before and after aconitine application for 0.5 h. GAPDH and β-actin were used as standards for analyses of the protein and total RNA samples, respectively. Data are presented as the mean ± S.E. Differences were considered statistically significant when  $p$ -value < 0.05,  $t$ -test,  $n = 4$ . (C) Immunostaining of RyR<sub>2</sub> fluorescence in CN and KD cardiomyocytes before and after aconitine application, respectively, using the anti-RyR primary antibody (scale bar: 50 μm). Immunofluorescence staining on cardiomyocytes RyR positive signals is better observed in the cytosol (green signals). All nuclei were stained with PI (CN, control; KD, knockdown; ACO, aconitine).**

contracture was done in 3 μM aconitine-containing perfusion solution for 5 min (CN cardiomyocytes: from  $164.25 \pm 33.29$  to  $254.17 \pm 35.41$  ΔF/F<sub>0</sub>%,  $p < 0.05$ ; KD cardiomyocytes: from  $83.89 \pm 28.36$  to  $178.26 \pm 29.32$  ΔF/F<sub>0</sub>%,  $p < 0.05$ , respectively) (Fig. 4C).

### 3.5. L-type Ca<sup>2+</sup> currents in cardiomyocytes were inhibited by aconitine

Current responses to a voltage step from -40 to 50 mV were recorded in control and RyR<sub>2</sub> KD cardiomyocytes and estimated as current density (A/F) (Fig. 5A and B). Both in

control and KD cardiomyocytes, I-V curves showed that activation of L-type Ca<sup>2+</sup> current began at -30 mV and peak currents occurred between 0 and +10 mV in the absence and presence of 3 μM aconitine (Fig. 5C and D).

Comparing the peak currents density at 10 mV, I-V relationships showed that L-type Ca<sup>2+</sup> currents in RyR<sub>2</sub> KD cardiomyocytes were higher than those in control cardiomyocytes ( $52.84 \pm 13.66$  A/F vs.  $75.77 \pm 18.80$  A/F). We can also see that both in control and RyR<sub>2</sub> KD cardiomyocytes, the L-type Ca<sup>2+</sup> current density at peak current was significantly lower in the presence of 3 μM aconitine as compared to that in the absence of aconitine (Fig. 5C and D). L-type Ca<sup>2+</sup> currents

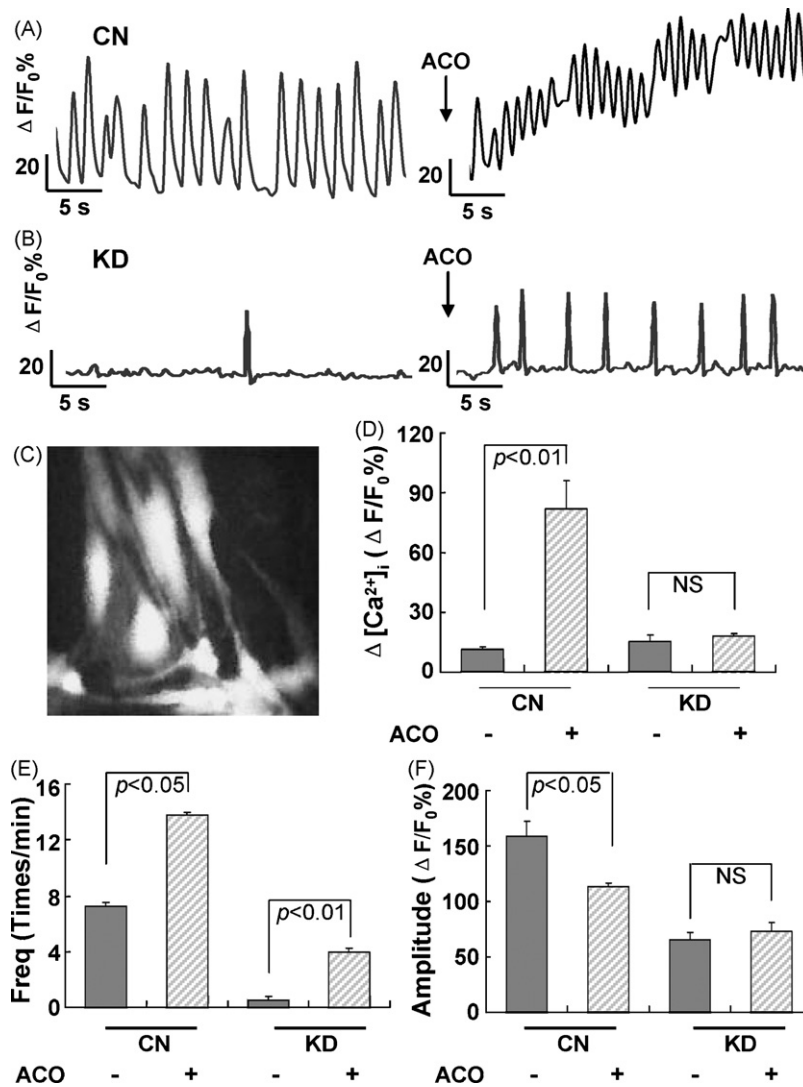


**Fig. 3** – Effects of aconitine on the relative intracellular  $\text{Ca}^{2+}$  concentration and spontaneous  $\text{Ca}^{2+}$  oscillations in control cardiomyocytes and knockdown cardiomyocytes (with siRNA3 transfection after 48 h) examined by  $\text{Ca}^{2+}$  imaging. (A and B) Representative recordings of the spontaneous  $\text{Ca}^{2+}$  oscillations in a given CN and KD cardiomyocyte before and after aconitine application, respectively. Traces indicate relative changes of fluo-3 intensity ( $\Delta F/F_0\%$ ) over time in cells randomly selected from the culture dish. Each trace represents  $\Delta F/F_0\%$  of an individual cell acquired every 5 s. (C) The photograph shows fluorescent image of cardiomyocytes loaded with fluo-3 AM (scale bar: 50  $\mu\text{m}$ ). (D–F) Effects of aconitine on the baseline  $[\text{Ca}^{2+}]_i$ , the frequency and amplitude of spontaneous  $\text{Ca}^{2+}$  oscillations in CN and KD cardiomyocytes before and after aconitine application. Data are presented as the mean  $\pm$  S.E. Differences were considered statistically significant when  $p$ -value  $< 0.05$ ,  $t$ -test,  $n = 4$  plates (CN, control; KD, knockdown; ACO, aconitine).

density in control cardiomyocytes was decreased by application of 3  $\mu\text{M}$  aconitine ( $52.84 \pm 13.66$  A/F vs.  $19.51 \pm 4.01$  A/F,  $p < 0.05$ ). And that in  $\text{RyR}_2$  KD cardiomyocytes was decreased from  $75.77 \pm 18.80$  to  $21.98 \pm 2.44$  A/F by application of 3  $\mu\text{M}$  aconitine ( $p < 0.05$ ) (Fig. 5E).

#### 4. Discussion

The present study established a model of  $\text{RyR}_2$  KD cardiomyocytes and found calcium homeostasis in these myocytes were seriously affected. In addition, we studied the possible role of

$\text{RyR}_2$  in aconitine-induced arrhythmias by comparing the effects of the presence and absence of aconitine in control cardiomyocytes and in cardiomyocytes with reduced  $\text{RyR}_2$  mRNA and protein levels. We concluded that alterations of  $\text{RyR}_2$  are important consequences of aconitine-stimulation and activation of  $\text{RyR}_2$  expression appear to have a direct relationship with aconitine-induced arrhythmias. This conclusion was mainly based on the observations that (1) aconitine induced up-regulation of  $\text{RyR}_2$  mRNA and protein levels both in control and  $\text{RyR}_2$  KD cardiomyocytes; (2) aconitine-induced recovery of spontaneous  $\text{Ca}^{2+}$  oscillations without affecting the baseline  $[\text{Ca}^{2+}]_i$  in  $\text{RyR}_2$  KD cardiomyocytes; (3) the level of

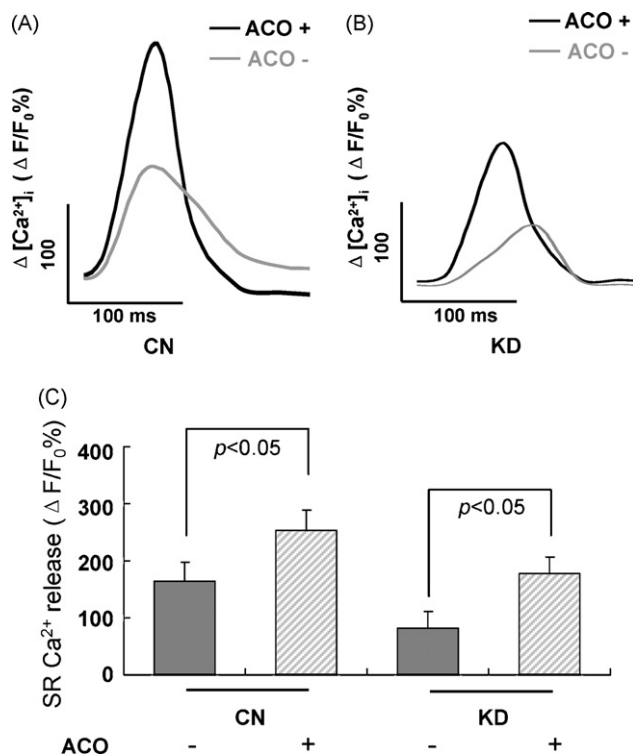


**Fig. 4 – Effects of aconitine on sensitivity to caffeine contracture in control cardiomyocytes and knockdown cardiomyocytes (with siRNA3 transfection after 48 h) examined by  $Ca^{2+}$  imaging. (A and B) Caffeine-induced  $Ca^{2+}$  transients in CN and KD cardiomyocytes before (gray trace) and after (black trace) aconitine application for 5 min. Each trace represents  $\Delta F/F_0\%$  of an individual cell acquired every 200 ms. (C) Average  $\Delta[Ca^{2+}]_i$  for caffeine-induced  $Ca^{2+}$  transients. Data are presented as the mean  $\pm$  S.E. Differences were considered statistically significant when  $p$ -value  $< 0.05$ ,  $t$ -test,  $n = 5$  cells per plate, four plates (CN, control; KD, knockdown; ACO, aconitine).**

caffeine-induced  $Ca^{2+}$  release in the cardiomyocytes was increased by aconitine; (4) L-type  $Ca^{2+}$  channel currents in cardiomyocytes were inhibited by aconitine. The present study therefore provides an insight into a useful method for preventing aconitine-induced arrhythmias by reducing  $Ca^{2+}$  leakage through the SR RyR<sub>2</sub> channel.

Mutations in the human RyR<sub>2</sub> gene have been shown to cause different forms of cardiac arrhythmias characterized by stress-, emotion-, and physical exercise-induced ventricular tachycardia (VT). However, the molecular and cellular mechanisms underlying these forms of ventricular arrhythmias are not clear [22]. It has been hypothesized that disease-associated RyR<sub>2</sub> mutations are likely to cause the channel to open spontaneously or to increase its sensitivity to activation by luminal  $Ca^{2+}$  [23,24]. In an earlier study we found that aconitine could enhance mRNA and protein levels of RyR<sub>2</sub> gene [7]. We conjectured, on these grounds, that alterations in RyR<sub>2</sub> channel function induced by aconitine would influence the properties of SR  $Ca^{2+}$  release and spontaneous  $Ca^{2+}$  oscillations, and thus cause the occurrence of triggered

arrhythmias. In order to elucidate the crucial role of RyR<sub>2</sub> in aconitine-induced arrhythmia, we use the RyR<sub>2</sub> gene KD cardiomyocytes model to further study the role of RyR<sub>2</sub> in aconitine-induced arrhythmic toxicity.

The siRNA method for reducing gene expression is a rapidly evolving tool in molecular biology. There are several methods for preparing siRNA [25]. Here, we report that reduction of RyR<sub>2</sub> gene expression can be obtained by the chemical synthesis siRNAs with the aid of lipid-based reagent for reverse transfection (Fig. 1). Moreover, RT-PCR shows a more pronounced reduction of RyR<sub>2</sub> mRNA level compared to protein expression by western blot. This finding is likely due to drastic interference and specific degradation of mRNA by siRNA, indicating that our procedure of RNA silencing is effective in neonatal rat cardiomyocytes.

It is known that  $[Ca^{2+}]_i$  occupies a key role in cardiac e-c coupling. During an action potential (AP), the influx of extracellular  $Ca^{2+}$  via L-type  $Ca^{2+}$  channels triggers SR  $Ca^{2+}$  release, resulting in an increase in  $[Ca^{2+}]_i$  and myofilament activation [26]. When SR  $Ca^{2+}$  content reaches a critical level, spontaneous SR  $Ca^{2+}$  release in the form of  $Ca^{2+}$  waves or  $Ca^{2+}$  oscillations occurs in cardiac cells [27]. The systolic dysfunction observed after transient  $Ca^{2+}$  overload is the result of both decreased systolic  $Ca^{2+}$  and reduced myofilament sensitivity to  $Ca^{2+}$  [28].

In our experiments, we tested the spontaneous  $Ca^{2+}$  oscillations and  $[Ca^{2+}]_i$  in control and RyR<sub>2</sub> KD cardiomyocytes with aconitine-stimulation (Fig. 3). We found that aconitine induced a sharp increase in the relative  $[Ca^{2+}]_i$  and aberrant spontaneous  $Ca^{2+}$  oscillations in control cardiomyocytes indicating that the malfunctions of spontaneous  $Ca^{2+}$  oscillations and the ability to contract and relax in aconitine-induced cardiomyocytes are due to  $Ca^{2+}$  overload of the cytosolic  $Ca^{2+}$  concentration. In RyR<sub>2</sub> KD cardiomyocytes with aconitine-stimulation, the spontaneous  $Ca^{2+}$  oscillations were recovered partly, also reflects the properties of RyR<sub>2</sub> in aconitine-induced cardiomyocytes. It has been suggested that the occurrence of  $Ca^{2+}$  oscillations in RyR<sub>2</sub> (wild type) cells depends completely on the expression of RyR<sub>2</sub> [27], which is consistent with our results that modulating RyR<sub>2</sub> function has a close relationship with the intracellular  $Ca^{2+}$  concentration and spontaneous  $Ca^{2+}$  oscillations in cardiomyocytes with aconitine-stimulation.

In order to verify whether the overload of the cytosolic  $Ca^{2+}$  concentration and the alteration of spontaneous  $Ca^{2+}$  oscillations were triggered by excess enhancement of the SR  $Ca^{2+}$  release in aconitine-induced cardiomyocytes, we investigated the level of caffeine-induced  $Ca^{2+}$  release in control and RyR<sub>2</sub> KD cardiomyocytes.

RyR<sub>2</sub> regulates SR  $Ca^{2+}$  release and thus, the  $Ca^{2+}$  content of SR luminal storage. We investigated the SR  $Ca^{2+}$  release by caffeine stimulation. Rapid application of caffeine solution induces a  $[Ca^{2+}]_i$  transient and contracture in cardiomyocytes, and the amplitude can be used as an index of SR  $Ca^{2+}$  releasable content [29]. Fig. 4 demonstrates that higher level of caffeine-induced  $Ca^{2+}$  release was observed in both control and RyR<sub>2</sub> KD cardiomyocytes with aconitine-stimulation. These data suggest that aconitine caused enhancing SR  $Ca^{2+}$  release by RyR<sub>2</sub> luminal  $Ca^{2+}$  activation and an increase in RyR<sub>2</sub> gene expression due to aconitine results in an increase in SR  $Ca^{2+}$  leak and intracellular  $Ca^{2+}$  concentration. It has been

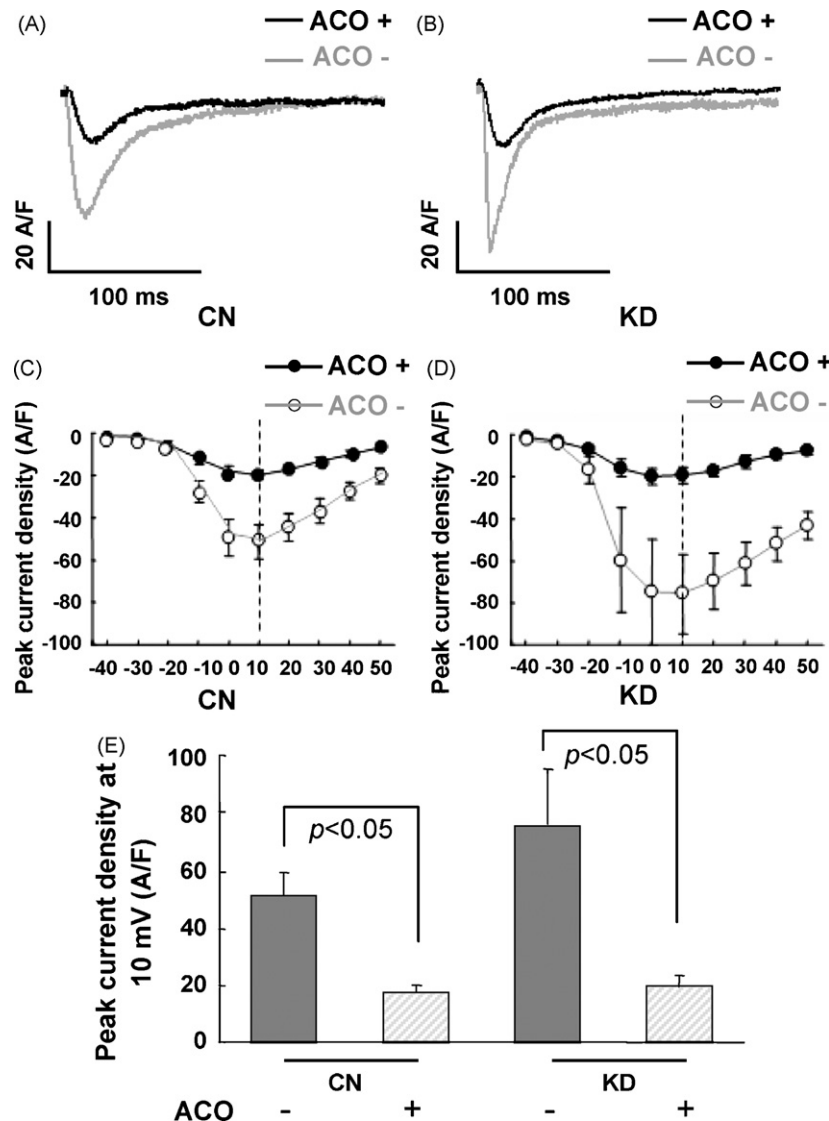


**Fig. 5** – Effects of aconitine on the L-type  $\text{Ca}^{2+}$  currents in control cardiomyocytes and knockdown cardiomyocytes (with siRNA3 transfection after 48 h) examined by patch clamp. (A and B) L-type  $\text{Ca}^{2+}$  currents recorded at 10 mV command potential in CN and KD cardiomyocytes before (gray trace) and after (black trace) aconitine application for 5 min. (C and D)  $I_{\text{Ca}}-V$  relationships in CN (hollow circle) and KD cardiomyocytes (solid circle) before (gray trace) and after (black trace) aconitine application. (E) Peak current density at 10 mV command potential in CN and KD cardiomyocytes. Data are presented as the mean  $\pm$  S.E. Differences were considered statistically significant when  $p$ -value  $< 0.05$ ,  $t$ -test,  $n = 5$  cells per plate, five plates (CN, control; KD, knockdown; ACO, aconitine).

shown that an increase in  $\text{RyR}_2$  activity lowered the amplitude of propagating  $\text{Ca}^{2+}$  waves, but increased the frequency of propagating  $\text{Ca}^{2+}$  waves and this increase escalates the propensity for triggered arrhythmia [23,24]. An increased propensity for spontaneous  $\text{Ca}^{2+}$  oscillations and decreased propagating  $\text{Ca}^{2+}$  waves under the condition of intracellular  $\text{Ca}^{2+}$  overload triggered by excess enhancement of the SR  $\text{Ca}^{2+}$  release may underlie a mechanism of aconitine-induced cardiac arrhythmia. It has now become clear that alterations in  $\text{RyR}_2$  channel function as a result of genetic defects can cause ventricular arrhythmias [30]. Our findings also provide evidence that acquired dysfunction of  $\text{RyR}_2$  could lead to arrhythmia susceptibility.

On the other hand, recent investigations show that SR  $\text{Ca}^{2+}$  release appears to modulate the sarcolemmal L-type  $\text{Ca}^{2+}$  currents, suggesting a retrograde communication from the SR to the sarcolemmal L-type  $\text{Ca}^{2+}$  channels in cardiac e-c coupling [31]. In this regard, it is worthy to identify the effect of aconitine on L-type  $\text{Ca}^{2+}$  currents in control and  $\text{RyR}_2$  KD cardiomyocytes.

As reported, aconitine binds to  $\text{Na}^+$  channels and prolongs the voltage-dependent  $\text{Na}^+$  channel open state, favoring entry of a large quantity of  $\text{Na}^+$  into cytosol. This influx then induces AP and activates the L-type  $\text{Ca}^{2+}$  currents [32]. In the present study, tetrodotoxin (TTX, 1  $\mu\text{M}$ ) was used to inhibit the effect of the  $\text{Na}^+$  channel activation induced by aconitine.



As shown in Fig. 5, compared with the control cardiomyocytes, the L-type  $\text{Ca}^{2+}$  currents were increased in RyR<sub>2</sub> KD cardiomyocytes. Moreover, application of aconitine resulted in a decrease in magnitude of the L-type  $\text{Ca}^{2+}$  currents in control and RyR<sub>2</sub> KD cardiomyocytes. The physiological function of the L-type current in skeletal muscle fibers is unclear. Some proposal reported that a depletion of SR  $\text{Ca}^{2+}$  would result in decreased SR  $\text{Ca}^{2+}$  release on plasma membrane depolarization, resulting in a smaller rise in triadic  $\text{Ca}^{2+}$ , which in turn would stimulate  $\text{Ca}^{2+}$  influx via the L-type  $\text{Ca}^{2+}$  channel [31]. Our results are consistent with the proposal that aconitine stimulation-induced SR  $\text{Ca}^{2+}$  leakage through RyR<sub>2</sub> channel, which depressed L-type  $\text{Ca}^{2+}$  current. Our results support the hypothesis of a retrograde communication between the SR  $\text{Ca}^{2+}$  release channel and the L-type  $\text{Ca}^{2+}$  channel (DHPR). This communication may be mediated in some cases by a direct interaction between the two channel proteins, L-type  $\text{Ca}^{2+}$  channel and RyR<sub>2</sub> [33].

## Acknowledgements

The authors want to thank Ms. Carlyn Tan from Northwestern University (Chicago) for her help in revising this manuscript. The present work was supported by grants of the 'Tenth-five' National Key Technologies R&D Programme (No. 2004BA721A11) and the Ph.D. Programs Foundation of Ministry of Education of China (No. 20060003036).

## REFERENCES

- [1] Sato H, Yamada C, Konno C, Ohizumi Y, Endo K, Hikino H. Pharmacological actions of aconitine alkaloids. *Tohoku J Exp Med* 1979;128:175–87.
- [2] Honerjager P, Meissner A. The positive inotropic effect of aconitine. *Naunyn Schmiedeberg Arch Pharmacol* 1983;322:49–58.
- [3] Hikino H, Konno C, Takata H, Yamada Y, Yamada C, Ohizumi Y. Anti-inflammatory principles of aconitum roots. *J Pharm Dyn* 1980;3:514–25.
- [4] Herzog W, Feibel R, Bryant S. The effect of aconitine on the giant axon of the squid. *J Gen Physiol* 1964;47:719–33.
- [5] Ameri A. The effects of Aconitum alkaloids on the central nervous system. *Prog Neurobiol* 1998;56:211–35.
- [6] Levy S, Breithardt G, Campbell RW, Camm AJ, Daubert JC, Allessie M, et al., Working Group on Arrhythmias of the European Society of Cardiology. Atrial fibrillation: current knowledge and recommendations for management. *Eur Heart J* 1998;19:1294–320.
- [7] Fu M, Wu M, Wang JF, Qiao YJ, Wang Z. Disruption of the intracellular  $\text{Ca}^{2+}$  homeostasis in the cardiac excitation-contraction coupling is a crucial mechanism of arrhythmic toxicity in aconitine-induced cardiomyocytes. *Biochem Biophys Res Commun* 2007;354:929–36.
- [8] Eisner DA, Choi HS, Diaz ME, O'Neill SC, Trafford AW. Integrative analysis of calcium cycling in cardiac muscle. *Circ Res* 2000;87:1087–94.
- [9] Bers DM. Cardiac excitation-contraction coupling. *Nature* 2002;415:198–205.
- [10] MacLennan DH, Kranias EG. Phospholamban: a crucial regulator of cardiac contractility. *Nat Rev Mol Cell Biol* 2003;4:566–77.
- [11] Fabiato A. Simulated calcium current can both cause calcium loading in and trigger calcium release from the sarcoplasmic reticulum of a skinned canine cardiac Purkinje cell. *J Gen Physiol* 1985;85:291–320.
- [12] Mickelson JR, Louis CF. Malignant hyperthermia: excitation-contraction coupling,  $\text{Ca}^{2+}$  release channel, and cell  $\text{Ca}^{2+}$  regulation defects. *Physiol Rev* 1996;76:537–92.
- [13] Loke J, MacLennan DH. Malignant hyperthermia and central core disease: disorders of  $\text{Ca}^{2+}$  release channels. *Am J Med* 1998;104:470–86.
- [14] Marx SO, Reiken S, Hisamatsu Y, Jayaraman T, Burkhoff D, Roseblit N, et al. PKA phosphorylation dissociates FKBP12.6 from the calcium release channel (ryanodine receptor): defective regulation in failing hearts. *Cell* 2000;101:365–76.
- [15] George CH, Higgs GV, Lai FA. Ryanodine receptor mutations associated with stress-induced ventricular tachycardia mediate increased calcium release in stimulated cardiomyocytes. *Circ Res* 2003;93:531–40.
- [16] Yang HT, Tweedie D, Wang S, Guia A, Vinogradova T, Bogdanov K, et al. The ryanodine receptor modulates the spontaneous beating rate of cardiomyocytes during development. *Proc Natl Acad Sci USA* 2002;99:9225–30.
- [17] Zahabi A, Deschepper CF. Long-chain fatty acids modify hypertrophic responses of cultured primary neonatal cardiomyocytes. *J Lipid Res* 2001;42:1325–30.
- [18] Temsah RM, Netticadan T, Chapman D, Takeda S, Mochizuki S, Dhalla NS. Alterations in sarcoplasmic reticulum function and gene expression in ischemic-reperfused rat heart. *Am J Physiol* 1999;277:H584–94.
- [19] Zhou C, Wen ZX, Shi DM, Xie ZP. Muscarinic acetylcholine receptors involved in the regulation of neural stem cell proliferation and differentiation in vitro. *Cell Biol Int* 2004;28:63–7.
- [20] Knollmann BC, Chopra N, Hlaing T, Akin B, Yang T, Etensohn K, et al. Casq2 deletion causes sarcoplasmic reticulum volume increase, premature  $\text{Ca}^{2+}$  release, and catecholaminergic polymorphic ventricular tachycardia. *J Clin Invest* 2006;116:2510–20.
- [21] Reppel M, Sasse P, Piekorz R, Tang M, Roell W, Duan YQ, et al. S100A1 enhances the L-type  $\text{Ca}^{2+}$  current in embryonic mouse and neonatal rat ventricular cardiomyocytes. *J Biol Chem* 2005;280:36019–28.
- [22] Bassani RA, Bassani JW, Bers DM. Mitochondrial and sarcolemmal  $\text{Ca}^{2+}$  transport reduce  $[\text{Ca}^{2+}]_i$  during caffeine contractures in rabbit cardiac myocytes. *J Physiol* 1992;453:591–608.
- [23] Jiang D, Xiao B, Zhang L, Chen SR. Enhanced basal activity of a cardiac  $\text{Ca}^{2+}$  release channel (ryanodine receptor) mutant associated with ventricular tachycardia and sudden death. *Circ Res* 2002;91:218–25.
- [24] Tiso N, Stephan DA, Nava A, Bagattin A, Devaney JM, Stanchi F, et al. Identification of mutations in the cardiac ryanodine receptor gene in families affected with arrhythmogenic right ventricular cardiomyopathy type 2 (ARVD<sub>2</sub>). *Hum Mol Genet* 2001;10:189–94.
- [25] Priori SG, Napolitano C, Tiso N, Memmi M, Vignati G, Bloise R, et al. Mutations in the cardiac ryanodine receptor gene (hRyR<sub>2</sub>) underlie catecholaminergic polymorphic ventricular tachycardia. *Circulation* 2001;103:196–200.
- [26] Seth M, Sumbilla C, Mullen SP, Lewis D, Klein MG, Hussain A, et al. Sarco(endo)plasmic reticulum  $\text{Ca}^{2+}$  ATPase (SERCA) gene silencing and remodeling of the  $\text{Ca}^{2+}$  signal mechanism in cardiac myocytes. *Proc Natl Acad Sci USA* 2004;101:16683–8.
- [27] Jiang D, Xiao B, Yang D, Wang R, Choi P, Zhang L, et al. RyR<sub>2</sub> mutations linked to ventricular tachycardia and sudden death reduce the threshold for store-overload-induced  $\text{Ca}^{2+}$  release (SOICR). *Proc Natl Acad Sci USA* 2004;101:13062–7.

- 
- [28] Holt E, Christensen G. Transient  $\text{Ca}^{2+}$  overload alters  $\text{Ca}^{2+}$  handling in rat cardiomyocytes: effects on shortening and relaxation. *Am J Physiol* 1997;273:H573–82.
- [29] Catterall WA, Trainer V, Baden DG. Molecular properties of the sodium channel: a receptor for multiple neurotoxins. *Bull Soc Pathol Exot* 1992;85:481–5.
- [30] Zhang XQ, Song J, Rothblum L, Lun M, Wang X, Ding F, et al. Overexpression of  $\text{Na}^+/\text{Ca}^{2+}$  exchanger alters contractility and SR  $\text{Ca}^{2+}$  content in adult rat myocytes. *Am J Physiol Heart Circ Physiol* 2001;281:H2079–88.
- [31] Balog EM, Gallant EM. Modulation of the sarcolemmal L-type current by alteration in SR  $\text{Ca}^{2+}$  release. *Am J Physiol* 1999;276:C128–35.
- [32] Sterling NW. Comparison of aconitine-modified human heart (hH1) and rat skeletal ( $\mu$ 1) muscle  $\text{Na}^+$  channels: an important role for external  $\text{Na}^+$  ions. *J Physiol* 2002;538:759–71.
- [33] Nakai J, Dirksen RT, Nguyen HT, Pessah IH, Beam KG, Allen PD. Enhanced dihydropyridine receptor channel activity in the presence of ryanodine receptor. *Nature* 1996;380:72–5.